

Thiol functionalised supports for controlled metal nanoparticle formation for improved C-C coupling

Matthew E. Potter,^{[a]*} Joshua J. M. Le Brocq,^[a] Alice E. Oakley,^[a] Evangeline B. McShane,^[a] Panashe M. Mhembere,^[a] Marina Carravetta,^[a] Bart D. Vandegehuchte^[b] and Robert Raja^{[a]*‡}

Dedicated to Prof. Andy Hor on the occasion of his 65th birthday for his distinguished contributions to organometallic materials and heterometallic catalysis

[a] Dr. M. E. Potter, J. J. M. Le Brocq, A. E. Oakley, E. B. McShane, Dr. M. Carravetta and Prof. R. Raja
Department of Chemistry
University of Southampton
Southampton, HANTS, SO17 1BJ
E-mail: M.E.Potter@soton.ac.uk and R.Raja@soton.ac.uk

[b] Dr. B. D. Vandegehuchte
Total Research & Technology Feluy
Zone Industrielle Feluy C
B-7181 Seneffe, Belgium

Supporting information for this article is given via a link at the end of the document

Abstract: The myriad applications of metal nanoparticle systems have individual demands on their size, shape and electronic states, demanding novel synthetic methods to optimise these properties. Herein we report our method of exploiting strong thiol-Pd binding as a precursor for forming small, uniform Pd nanoparticles on activation. We validate our approach with a range of characterisation techniques and contrast our design strategy with an analogous wetness impregnation method, showing the drastic improvements for catalytic C-C coupling. The presence of the thiol groups offers greater control over nanoparticle formation, particularly temperature resolution on activation, potentially allowing more targeted nanoparticle formation procedures.

Metal nanoparticles (NPs) are at the forefront of modern technology in the fields of chemistry,^[1] optics^[2] and medicine,^[3] leading the way in applications such as drug delivery, imaging and catalysis.^[1a, 2-3] The interest in metal NPs is due to their small size, prompting a range of unique behaviours and properties not seen in the bulk material.^[4] Principally, this is due to the enhanced surface-to-volume ratio of nanoparticles, maximising the exposed 'frustrated surface', resulting in defect sites and different crystallographic planes.^[5] In catalysis this maximises the surface coverage of active sites that can initiate or propagate a vast range of chemical processes.^[6] Metal NPs are widely used as catalysts due to the many controllable parameters that can be tailored for specific functions, which includes nanoparticle size, shape, phase and composition.^[7] One of the challenges of using NPs is preventing agglomeration or sintering, as this typically leads to larger, less active species. To prevent this, NPs are commonly deposited onto porous supports with high surface areas, to both isolate and anchor the NPs, extending their lifetime.^[8] Because of the many tuneable NP parameters, a wide range of distinct synthetic techniques have been developed to deposit metal NPs onto solid supports, with varying complexity and efficacy.^[8c, 9] Wetness impregnation is still among the most widely used methods, due to its simplicity. However more precise methods of creating NPs have been developed,

including anchoring pre-formed metal clusters.^[9b] Organic moieties are increasingly being used to control the size and modify the electronic properties of metal NPs. Thiols, in particular, have been widely used due to their ability to form strong bonds with heavy metal atoms, making them excellent candidates for metal adsorption systems.^[10] Thiols have previously been used as capping agents, as the thiol-metal bonds hinder nanoparticle growth, limiting the NP size, where the metal-thiol bonds are typically much stronger than those seen in non-thiol based surfactants.^[11] This has been used to great effect in forming atomically precise metal clusters, such as Au₁₃ or Ag₄₄, and for tethering pre-made metal nanoparticles onto thiol-functionalised supports.^[10a, 10b] However there are scarce few reports where thiol-functionalised supports have been used for nanoparticle formation.^[10] In this work we exploit strong Pd-thiol interactions, by anchoring Pd atoms onto thiol-modified mesoporous silica, forming isolated Pd-thiol complexes. These systems can then be activated, giving small defined nanoparticles with a narrow size distribution.

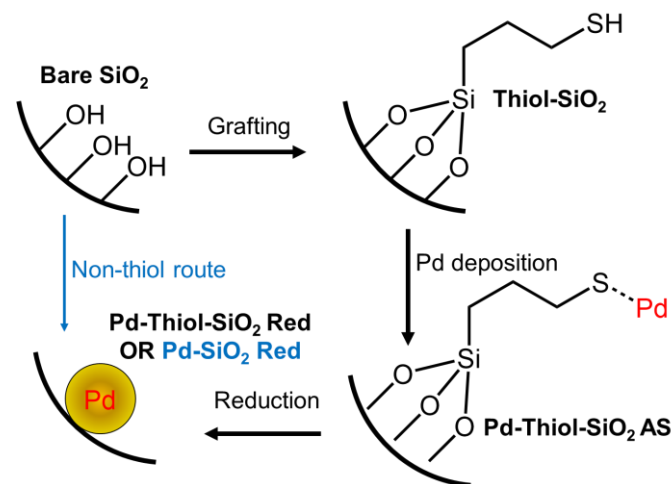


Figure 1. Schematic showing the different synthetic routes in this work.

We show that these systems offer superior catalytic activity for C-C bond formation through Suzuki Coupling (Figure S1), compared to identically prepared systems, without a thiol-binder. The benefit of the tethered thiol species is then explored by comparing analogous samples both with and without thiols, in a combined catalysis and characterisation study.

The parent material “Thiol-SiO₂” was prepared by grafting 0.3 mmol⁻¹ 3-mercaptoptrimethoxysilane onto mesoporous silica (see ESI for details). The integrity of the grafted thiols was confirmed using ¹³C solid-state NMR (Figure 2),^[12] with elemental analysis showing the expected C/S molar ratio of 3 (Table S1). Low thiol loadings were purposefully used to disperse the thiols within the non-passivated 150 Å mesoporous silica support (~150 Å²thiol⁻¹), encouraging isolated metal complexes to form. Grafting thiol onto silica maintained the porosity (Figure S2 and Table S2), resulting in a 10 % reduction in both pore volume and surface area, with a subtle increase in the average pore size, on grafting the thiol groups. As expected, there was little change in the visible region of the UV/Vis spectra (Figure S3).

Pd (K₂PdCl₄) was mixed in solution with “Thiol-SiO₂” at room temperature, forming Pd-S bonds, making the “Pd-Thiol-SiO₂ AS” system. Adding Pd did not affect the porosity, with pore volume, width and surface area matching the parent “Thiol-SiO₂” system (Figure S2 and Table S2). The UV/Vis spectra dramatically changed on adding Pd, as the powder changed colour from white to orange (Figure S3). TEM images showed no evidence of metallic particles or clustering (Figure S4), supporting the formation of isolated, single atom Pd complexes throughout the system. ¹³C NMR (Figure 2) confirms the binding behaviour further, with the “Thiol-SiO₂” ¹³C NMR showing two signals, with the dominant signal at 28 ppm (both SiCH₂-CH₂-SH and SiC₂H₄-CH₂-SH) and a smaller signal at 10 ppm (Si-CH₂-C₂H₅-SH), as expected.^[12] On binding to the Pd²⁺ (Pd-Thiol-SiO₂ AS) the SiCH₂H₄-CH₂-SH signal moved to a higher chemical shift (49 ppm), with the other two carbons largely unchanged. This mirrors behaviour seen with grafted thiols binding to mercury atoms.^[12] It is noted the “Pd-Thiol-SiO₂ AS” system required 10 times more scans to reach an equivalent signal to noise ratio as the “Thiol-SiO₂” system, likely due to the electron spin from the unpaired electrons in the Pd²⁺ present.

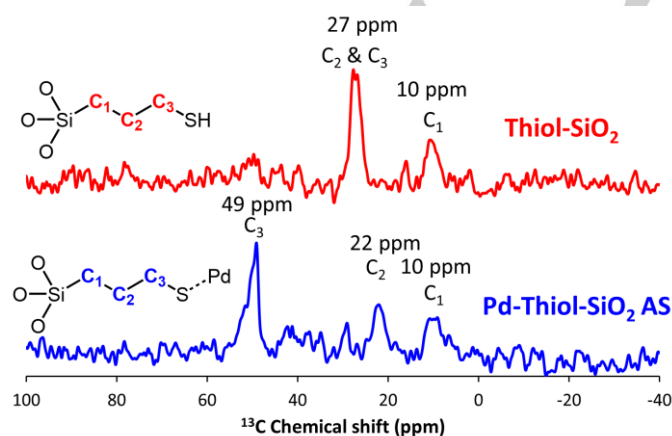


Figure 2. Showing the influence of Pd binding to grafted-thiols with ¹³C solid state NMR.

“Pd-Thiol-SiO₂ AS” was reduced under a hydrogen flow forming “Pd-Thiol-SiO₂ Red”, prompting a further colour change from orange to brown, with further changes in the UV/Vis spectra. Most notably a broad feature between 375 – 485 nm is present, matching previous assignments of a combination of LMCT and d-d transitions for square planar Pd²⁺ species.^[13] Reduction caused minimal changes in porosity, again the surface area, pore volume and width were in good agreement with the parent systems (Figure S2 and Table S2). Elemental analysis showed that 29 % of the thiol species had been removed on reduction, though the C/S ratio was largely maintained (Table S1). The ¹³C NMR of “Pd-Thiol-SiO₂ Red” shows that the 49 ppm signal from the “Pd-Thiol-SiO₂ AS” remains, but there is now a dominant signal at 16 ppm (Figure S5). This confirms the thiol group has also been affected by the reduction process, and this new signal is possibly the result of H₂S removal, leaving an alkyl chain, or thiol-ether formation.^[14]

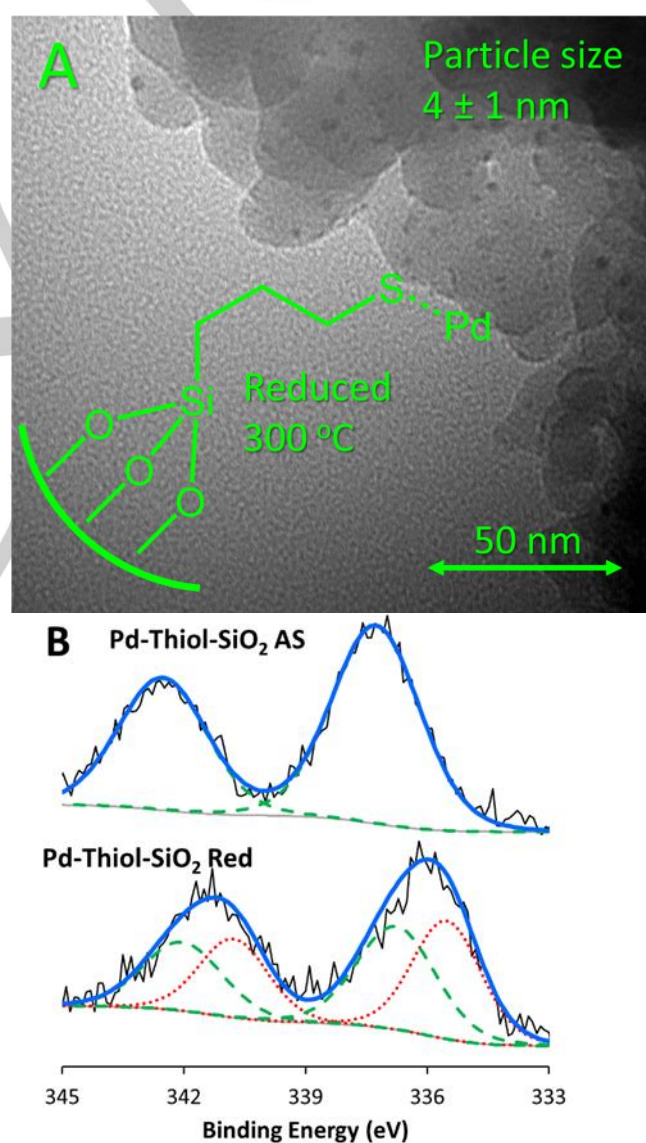


Figure 3. TEM image (A) showing the small, uniform Pd nanoparticles of the “Pd-Thiol-SiO₂ Red” system, and the corresponding XPS spectra (B) showing the total fit (blue, thick), experimental data (black, thin), background (grey, thin), Pd²⁺ (green, dashed) and Pd⁰ (red, dots) contributions.

ICP analysis showed the Pd content was 0.76 wt%, corresponding to a distribution of $642 \text{ \AA}^2\text{Pd}^{-1}$. TEM confirmed the formation of small, uniform Pd nanoparticles, with an average diameter of $4 \pm 1 \text{ nm}$ (Figures 3A and S6). XPS shows the influence of reducing the materials, with the “Pd-Thiol-SiO₂ AS” spectra shows just two signals at 342.6 and 337.1 eV, corresponding to Pd²⁺ 3d_{3/2} and 3d_{5/2} transitions, confirming Pd primarily exists as Pd²⁺, bound to the thiol species (Figure 3B).^[15] Post-reduction, the XPS signals of “Pd-Thiol-SiO₂ Red” have both shifted to lower binding energies (341.2 and 366.0 eV), which are due to a combination of Pd²⁺ and Pd⁰ contributions.^[15] Therefore this data has been fit using roughly even quantities of Pd²⁺ (3d_{3/2} and 3d_{5/2} at 342.1 and 336.9 eV) and Pd⁰ (3d_{3/2} and 3d_{5/2} at 340.7 and 335.5 eV), suggesting some Pd is still existing as Pd²⁺ and has not fully extruded from the thiol groups (Figure 3B), due to the strong binding interactions.

To explore the influence of the anchoring thiol species, an analogous synthesis procedure was used with bare SiO₂ instead of “Thiol-SiO₂”, doping equivalent amounts of Pd “Pd-SiO₂ AS”, and reduced under the same conditions “Pd-SiO₂ Red”. Introducing Pd directly onto the mesoporous SiO₂ support (0.96 wt%) subtly reduced the pore volume and surface area, though prompted a noticeable change in pore width from 188 to 227 Å, which was maintained on reduction (Figure S7 and Table S3). It is noted that the porosity of the “Pd-Thiol-SiO₂ Red” and “Pd-SiO₂ Red” is near identical (Tables S2 & S3), thus any differences in behaviour are not due to porosity. The Pd metal loadings are also similar, with “Pd-SiO₂ Red” having slightly more Pd (0.96 wt%) than “Pd-Thiol-SiO₂ Red” (0.76 wt%). The two systems are similar in colour, reflected in the agreement in their UV/Vis spectra (Figure S8), both showing a sharp peak at 237 nm, shifting the bare SiO₂ signal. The Pd-SiO₂ AS also shows features at 285 and 426 nm, again attributed to a combination of LMCT and d-d transitions.^[13] TEM images of “Pd-SiO₂ Red” show significantly larger Pd particles, with much larger variation in particle size, with diameters of $23 \pm 12 \text{ nm}$ (Figures 4 and S9).

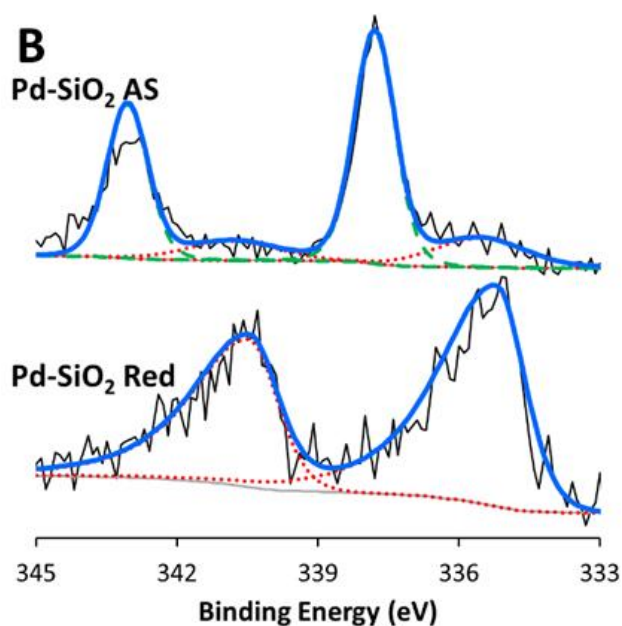
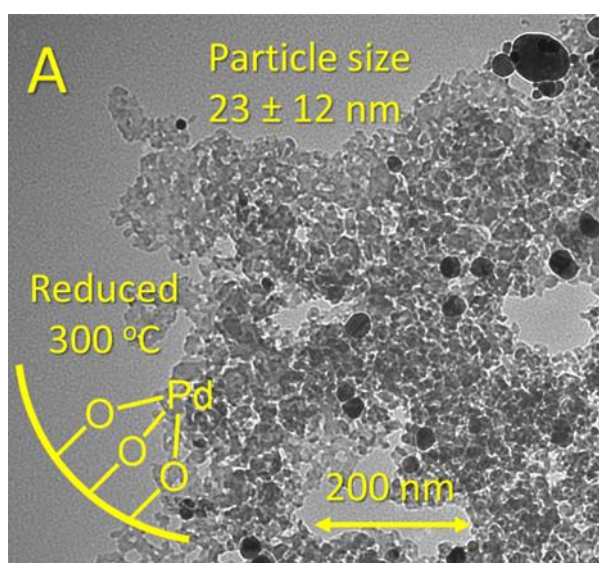
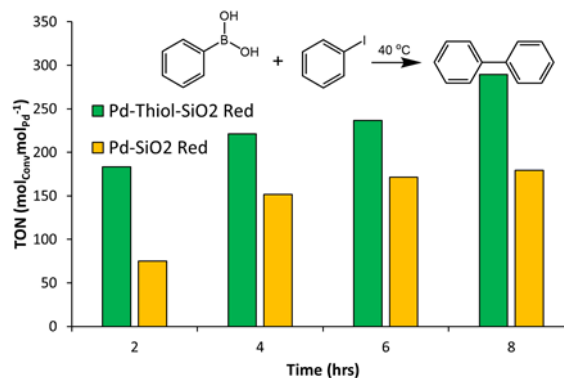


Figure 4. TEM image (A) showing large Pd nanoparticles in the “Pd-SiO₂ Red” system, and the corresponding XPS spectra (B) showing the total fit (blue, thick), experimental data (black, thin), background (grey, thin), Pd²⁺ (green, dashed) and Pd⁰ (red, dots) contributions. Contrasted with Figure 3, this shows the influence of the thiol groups.

The significant difference in Pd nanoparticle size is unlikely to be due to difference in Pd loadings (0.76 wt% v 0.96 wt%), instead the thiol-groups likely had the intended effect of separating individual Pd atoms, increasing dispersion, which lead to smaller more active sites. This, combined with improved Pd distribution throughout the sample, made the metal atoms less mobile during activation, leading to smaller metallic nanoparticles. XPS confirms that “Pd-SiO₂ AS” contains mostly Pd²⁺, with a small contribution from Pd⁰, as expected.^[15] On reduction this is quantitatively reduced to Pd⁰ (Figure 4B). Therefore, the inclusion of thiol groups allows more control over the reduction process, by giving access to a much wider temperature range to form nanoparticles.

Figure 5. Suzuki Coupling catalytic data, showing the catalytic benefits of



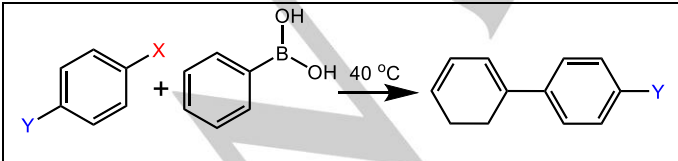
thiol-group grafting. Reaction conditions: 40 °C, 50 mg of catalyst, 0.94 mmol of phenylboronic acid, 0.86 mmol of naphthalene (internal standard), 0.87 mmol of anhydrous K₂CO₃, 1.22 mmol of iodobenzene and 15 mL of ethanol.

The influence of the thiol group was examined by comparing the catalytic turnover numbers (TONs) of the two reduced Pd species, for the Suzuki coupling of iodobenzene and phenylboronic acid (Figures 5 and S10). After 2 hours the turnover frequency (TOF), and rate of reaction, for the "Pd-Thiol-SiO₂ Red" species (92 hr⁻¹) was over twice that of the "Pd-SiO₂ Red" species (38 hr⁻¹), due to the superior catalytic performance (yield of 70 mol% v 39 mol% respectively) of the "Pd-Thiol-SiO₂ Red" catalyst. This improved activity was maintained over a sustained time period, further vindicating the stability of the catalyst and its catalytic resilience. It is likely that the thiols still present in the activated system, help anchor the metal nanoparticles, preventing leaching and agglomeration, or possibly also enabling 'catch-and-release' chemistry. We note that the activity in this reaction is purely due to the Pd species, as the control "Thiol-SiO₂" system showed no activity after 8 hours. The improved activity and efficiency of the thiol system is primarily attributed to the smaller Pd nanoparticles in the thiol-based system. This has two benefits; as smaller nanoparticles geometrically provide a greater fraction of exposed Pd sites, available for reaction, leading to a higher proportion of reaction sites. Similarly, for particles less than 3 nm, the electronic properties are notably different to 'bulk' metals. It is also possible that the Pd-S bonding may increase the systems activity, though this will depend on what the prevailing mechanism of this reaction is. However, the organic nature of the thiol-group makes them open to subtle modifications to probe these theories in future.

To determine the stability of the system the "Pd-Thiol-SiO₂-Red" catalyst was recovered after 8 hours of a Suzuki coupling reaction between iodobenzene and phenyl boronic acid. The used catalyst was filtered from the reaction mixture, dried and reactivated and retested under identical reaction conditions (Figure S11). Very little deviation was observed between the TON's of the "Fresh" and "Recycled" systems after 4 hours, but a slight dip was seen after 8 hours. Overall though the activity is largely the same, showing the stability of our system.

To confirm the superior activity of our thiol-based system; "Pd-Thiol-SiO₂-Red" over the standard "Pd-SiO₂-Red" system we explored a wider range of substrates, varying the nature of the halogenated benzene system for coupling to phenyl boronic acid (Table 1).

Table 1. Suzuki Coupling catalytic data, showing the benefit of thiol-group grafting with a range of substrates. Reaction conditions: 40 °C, 50 mg of catalyst, 0.94 mmol of phenylboronic acid, 0.86 mmol of naphthalene (internal standard), 0.87 mmol of anhydrous K₂CO₃, 1.22 mmol of halogenated benzene and 15 mL of ethanol.



Entry	X	Y	Time (hrs)	TON of Pd-Thiol-SiO ₂ -Red (mol _{conv} /molPd ⁻¹)	TON for Pd-SiO ₂ -Red (mol _{conv} /molPd ⁻¹)
1	I	H	2	183	75
2	I	NO ₂	2	202	178
3	Br	H	4	145	135
4	Cl	H	8	37	< 5

In all four cases (Table 1) the thiol-based system ("Pd-Thiol-SiO₂-Red") outperformed the more traditional system ("Pd-SiO₂-Red"), showing the versatility of our system. The performance of our system mimics previous findings in the literature,^[16] with the 1-iodo-4-nitro-benzene substrate (Entry 2), being more active than the iodobenzene analogue (Entry 1). Similarly, the bromobenzene (Entry 3) and chlorobenzene (Entry 4) were found to be successively less active than iodobenzene substrate, as seen by the lower TONs, even over longer time periods, again as previously seen in the literature. Despite this the thiol-based system consistently showed better activity than the traditional system, verifying our approach.

Contrasting the efficacy of our systems with other recent systems in the literature (Table S4) shows that we can achieve comparable TOF values with our "Pd-Thiol-SiO₂-Red" system. While some systems have achieved TOFs that are an order of magnitude larger than ours, these are typically done at elevated temperatures, and the result of a catalytic studies to optimise reaction conditions. As such our current values should be taken as a lower-limit of what these systems are able to achieve.

In this work we have shown that thiol groups, anchored onto silica are effective binding sites for Pd atoms, which when reduced, trigger the formation of small nanoparticles with a narrow size distribution. This approach led to catalysts with superior activity over analogous systems prepared using conventional techniques, attributed to the smaller metal nanoparticles. Our approach of forming the nanoparticles on the support, instead of anchoring them post-synthetically, has the benefit that there are many controllable variables that could be modulated to improve the activity of the system. This includes the distribution of the initial binding sites, reduction temperature and the precise nature of the thiol groups. As such this approach has the potential to be applied to a wide range of metal-doped porous catalysts for mechanistic studies and optimising catalytic reactivity.

Acknowledgements

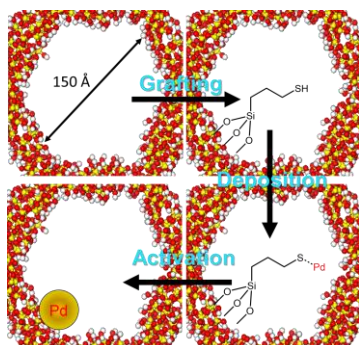
MEP, JJMLB, AEO, EBM, MC and RR acknowledge the Total "Consortium on Metal Nanocatalysis" project for funding. PMM acknowledges AdvanSix and Honeywell LLC for financial support. The TEM images were measured at Bioimaging Unit, University Hospital Southampton with the assistance of Patricia M. Goggin. We acknowledge EPSRC National Facility, HarwellXPS for XPS data collection.

Keywords: keyword 1 • keyword 2 • keyword 3 • keyword 4 • keyword 5

- [1] a) Z. Li, S. Ji, Y. Liu, X. Cao, S. Tian, Y. Chen, Z. Niu, Y. Li, *Chem Rev* **2020**, *120*, 623-682; b) S. Mavila, I. Rozenberg, N. G. Lemcoff, *Chem. Sci.* **2014**, *5*, 4196-4203; c) M. L. Kahn, A. Glaria, C. Pages, M. Monge, L. Saint Macary, A. Maisonnat, B. Chaudret, *Journal of Materials Chemistry* **2009**, *19*.
- [2] I. Venditti, *Materials (Basel)* **2017**, *10*.
- [3] X. Han, K. Xu, O. Taratula, K. Farsad, *Nanoscale* **2019**, *11*, 799-819.
- [4] a) V. Amendola, R. Pilot, M. Frascioni, O. M. Marago, M. A. Iati, *J Phys Condens Matter* **2017**, *29*, 203002; b) E. M. Dietze, P. N. Plessow, F. Stedt, *The Journal of Physical Chemistry C* **2019**, *123*, 25464-25469.

- [5] a) C. J. Kliewer, C. Aliaga, M. Bieri, W. Huang, C. K. Tsung, J. B. Wood, K. Komvopoulos, G. A. Somorjai, *J Am Chem Soc* **2010**, *132*, 13088-13095; b) C. Li, X. Han, F. Cheng, Y. Hu, C. Chen, J. Chen, *Nat Commun* **2015**, *6*, 7345.
- [6] S. Guo, S. Zhang, S. Sun, *Angew Chem Int Ed Engl* **2013**, *52*, 8526-8544.
- [7] a) S. M. Rogers, C. R. A. Catlow, C. E. Chan-Thaw, A. Chutia, N. Jian, R. E. Palmer, M. Perdjon, A. Thetford, N. Dimitratos, A. Villa, P. P. Wells, *ACS Catalysis* **2017**, *7*, 2266-2274; b) N. Dimitratos, A. Villa, L. Prati, C. Hammond, C. E. Chan-Thaw, J. Cookson, P. T. Bishop, *Applied Catalysis A: General* **2016**, *514*, 267-275.
- [8] a) T. W. van Deelen, C. Hernández Mejía, K. P. de Jong, *Nature Catalysis* **2019**, *2*, 955-970; b) B. Donoeva, N. Masoud, P. E. de Jongh, *ACS Catal* **2017**, *7*, 4581-4591; c) J. M. Campelo, D. Luna, R. Luque, J. M. Marinas, A. A. Romero, *ChemSusChem* **2009**, *2*, 18-45.
- [9] a) N. J. Costa, L. M. Rossi, *Nanoscale* **2012**, *4*, 5826-5834; b) R. D. Adams, M. Chen, G. Elpitiya, M. E. Potter, R. Raja, *ACS Catalysis* **2013**, *3*, 3106-3110; c) J. A. Lopez-Sanchez, N. Dimitratos, C. Hammond, G. L. Brett, L. Kesavan, S. White, P. Miedziak, R. Tiruvalam, R. L. Jenkins, A. F. Carley, D. Knight, C. J. Kiely, G. J. Hutchings, *Nat Chem* **2011**, *3*, 551-556; d) J. Zhang, L. Wang, Y. Shao, Y. Wang, B. C. Gates, F. S. Xiao, *Angewandte Chemie* **2017**, *129*, 9879-9883.
- [10] a) J. A. Larsson, M. Nolan, J. C. Greer, *The Journal of Physical Chemistry B* **2002**, *106*, 5931-5937; b) L. G. AbdulHalim, S. Ashraf, K. Katsiev, A. R. Kirmani, N. Kothalawala, D. H. Anjum, S. Abbas, A. Amassian, F. Stellacci, A. Dass, I. Hussain, O. M. Bakr, *Journal of Materials Chemistry A* **2013**, *1*; c) G. Bjorklund, G. Crisponi, V. M. Nurchi, R. Cappai, A. Buha Djordjevic, J. Aaseth, *Molecules* **2019**, *24*; d) T. Kang, Y. Park, J. Yi, *Industrial & Engineering Chemistry Research* **2004**, *43*, 1478-1484.
- [11] S. Campisi, M. Schiavoni, C. Chan-Thaw, A. Villa, *Catalysts* **2016**, *6*.
- [12] H. M. Kao, L. P. Lee, A. Palani, *Anal Chem* **2008**, *80*, 3016-3019.
- [13] A. Samanta, R. N. Devi, *ChemCatChem* **2013**, *5*, 1911-1916.
- [14] Y. Zhao, A. K. Steiger, M. D. Pluth, *J Am Chem Soc* **2019**, *141*, 13610-13618.
- [15] a) S. Alijani, S. Capelli, S. Cattaneo, M. Schiavoni, C. Evangelisti, K. M. H. Mohammed, P. P. Wells, F. Tessore, A. Villa, *Catalysts* **2019**, *10*; b) P. Verma, M. E. Potter, A. E. Oakley, P. M. Mhembere, R. Raja, *Nanomaterials (Basel)* **2021**, *11*.
- [16] P. Verma, Y. Kuwahara, K. Mori, H. Yamashita, *J Mater Chem A* **2016**, *4*, 10142-10150.

Entry for the Table of Contents



Isolated thiol-Pd complexes, grafted to mesoporous silica, serve as precursors for nanoparticle formation. This approach has several benefits over analogous impregnation methods, as we show that the thiol-groups, lead to smaller nanoparticles. This unique method to synthesise Pd-catalysts offers improved activity over analogous non-thiol systems, offering new opportunities to modulate and tailoring metal nanoparticles systems.